Grazing-incidence antireflection films. III. General theory for pure nuclear reflections

J. P. Hannon and G. T. Trammell
Physics Department, Rice University, Houston, Texas 77251

M. Mueller, E. Gerdau, R. Rüffer, and H. Winkler
II. Institut für Experimentalphysik, Universität Hamburg, D-2000 Hamburg 50, Federal Republic of Germany
(Received 9 May 1984; revised manuscript received 28 January 1985)

Very pure coherent nuclear reflections of γ rays can be obtained by grazing-incidence reflection from a mirror coated with a grazing-incidence antireflection film where either the mirror or one or more of the coating films are resonant. The nonresonant electronic reflection is strongly suppressed by destructive interference, while for near-resonance radiation, the index of refraction in the resonant medium is quite different from that for nonresonant radiation giving an impedance mismatch, and strong reflection occurs. Typically, it should be possible to suppress the nonresonant reflection to $\approx 10^{-4}$–10^{-3}, while maintaining resonant reflectivities of ≈ 0.7 with frequency half-widths which are strongly broadened to $\Gamma_{\text{eff}} \gtrsim 20\Gamma$ by the refraction-augmented "enhancement effect." This paper develops the general theory for pure nuclear reflections using grazing-incidence antireflection films, and treats in detail the case of a resonant mirror coated with a nonresonant impedance-matched quarter-wave film.

I. INTRODUCTION

Coherent scattering of γ rays by nuclei has received extensive theoretical and experimental effort since the discovery of the Mössbauer effect.[1–11] The first theoretical treatment of γ-ray optics was given by Trammell[1,2] in 1960, and concurrently the first dynamical experiments were performed by Black and Moon[3] on Bragg reflection of resonant γ rays, and by Bernstein and Campbell[4] on grazing-incidence reflection of γ rays by a resonant medium. Further important theoretical developments and detailed treatments of the dynamical theory have been given by Afanas'ev, Kagan, and co-workers,[5–7] and by Hannon and Trammell.[8–10]

Particular attention has been given to methods of suppressing the electronic scattering to obtain very pure nuclear reflections with high reflectivity. This can be accomplished with pure nuclear Bragg reflections by utilizing the unique features of the resonant nuclear scattering: (1) The strength of the resonant scattering can greatly exceed that of the electronic scattering, and the scattering is isotropic (except for the multipole pattern). For example, an unsplit ^{57}Fe nucleus scatters as 440 electrons at the 14.4-keV resonance, while the electronic scattering is 26 electrons in the forward direction, dropping off to 7.6 electrons at 90°. Consequently, very pure nuclear Bragg reflections can be obtained from crystalline thin films approximately several thousand angstroms thick, which are optically thick for the resonant scattering but essentially transparent for the electronic scattering.[12] (2) The resonant scattering depends on the direction of the magnetic field and electric field gradient (EFG) at the nucleus, while the x-ray scattering is insensitive to internal fields, so magnetic superlattice Bragg reflections are possible in antiferromagnetic crystals.[1,13–16] EFG superlattice reflections have also been observed.[16,17] (3) The nuclear transitions are multipole oscillators which (excluding unsplit E1 transitions) have a quite different polarization response than the electronic system, which scatters essentially as an isotropic $E1$ oscillator. For a 90° scattering with $\mathbf{k}_f$ in the direction of the incident *linear* polarization $\hat{\epsilon}_0$, the electronic scattering vanishes, while there will generally be strong resonant scattering, so very pure nuclear reflections can be obtained by 90° Bragg reflection of linearly- (π-) polarized γ rays.[12] (4) In complex systems with several atoms per unit cell, including ^{57}Fe, pure nuclear reflections can be obtained at special Bragg reflections where the unit-cell structure factor "accidentally" vanishes due to destructive interference.[18]

The purpose of this paper is to discuss a new non-Bragg technique for obtaining very pure nuclear reflections by grazing-incidence reflection from mirrors coated with grazing-incidence antireflection (GIAR) films,[19,20] where either the mirror or one or more of the coating films are resonant.

For example, a very pure nuclear reflection can be obtained by coating a resonant ^{57}Fe mirror with an impedance-matched quarter-wave film which strongly suppresses the nonresonant x-ray reflection, just as in optical coating of lenses. That is, we take a "quarter-wave film" on top of the ^{57}Fe surface, of proper impedance such that the x-ray reflection amplitudes at the upper and lower interfaces are equal, $R_{01}=R_{12}$, and with the thickness chosen so that the reflected waves arising from the two interfaces emerge 180° out of phase. However, for near-resonance radiation, the index of refraction in medium 2 is quite different from that for nonresonant radiation, giving an impedance mismatch, $R_{12}\neq R_{01}$, and strong reflection occurs. We will see, in fact, that in optimal cases it is possible to reduce the nonresonant reflectivity to $|R|^2_{\text{x ray}} \approx 10^{-4}$–$10^{-3}$, while maintaining a

resonant reflectivity $|R|_\gamma^2 \gtrsim 0.7$, with a strongly broadened width for the resonance response, $\Gamma_{\text{eff}} \gtrsim 20\Gamma$.

The strong resonance broadening is due to the refraction-augmented "enhancement effect." First there is a broadening $\approx \lambda\bar{n}\sigma_0\Gamma/2\phi^2 \approx 5\Gamma$ due to the "enhancement effect" of Trammell:[1,9] For waves incident near Bragg or grazing incidence on a resonant medium there is a broadened width to the frequency response due to coherent reemission into the reflection channel, and, correspondingly, the time response for coherent scattering is sped up relative to the natural lifetime for incoherent decay and internal conversion absorption. Secondly, there is an augmentation of "enhancement" by $[1-(\phi_c/\phi)^2]^{-1} \approx 4x$, where ϕ_c is the critical reflection angle: Because of refraction, the effective incidence angle of the wave driving the resonant system is decreased from ϕ to $\phi' = \phi[1-(\phi_c/\phi)^2]^{1/2}$, which, in turn, augments the enhancement broadening.

This paper is organized as follows: In Sec. II we summarize the main features of grazing-incidence reflection from a single resonant medium. In Sec. III we then treat resonant reflection from a stratified medium in which one or more of the layers or substrate mirror are resonant. In Sec. IV we give a detailed treatment of pure nuclear reflection from a resonant mirror coated with a nonresonant impedance-matched quarter-wave film, and also briefly mention alternate thin-film techniques for pure nuclear reflections.

The application to synchrotron filtering is treated in the following paper (paper IV),[21] and a detailed treatment of alternate thin-film techniques for pure nuclear reflections will be given in a subsequent paper.[22]

II. REFLECTION FROM A RESONANT MEDIUM

In this section we summarize the main features of grazing-incidence reflection from a resonant medium. Aspects of the theory have been treated by Trammell,[1] Bernstein and Campbell,[4,23] and Hannon and Trammell,[9,10] and experimental investigations have been carried out by Bernstein and Campbell[4] and by Wagner.[24]

A complicating, but interesting feature of γ-ray optics is the presence of strong optical activity, which gives strong polarization mixing (i.e., orthogonal scattering $\hat{\epsilon}_x \leftrightarrow \hat{\epsilon}_y$) and Faraday-type effects.[9,10,25,26]

The eigenpolarizations $\hat{\epsilon}_\eta$, $\eta = \text{I,II}$, for propagation through the medium and for critical reflection, are determined by the eigenvalue equation

$$\tilde{f}\hat{\epsilon}_\eta = f_\eta \hat{\epsilon}_\eta \ , \tag{1}$$

where $\tilde{f}$ is the 2×2 forward-scattering amplitude matrix

$$\tilde{f} = \begin{bmatrix} f_{xx} & f_{xy} \\ f_{yx} & f_{yy} \end{bmatrix} . \tag{2}$$

Here, f_{ab} ($a,b = x$ or y) is the coherent elastic forward-scattering amplitude for scattering $\hat{\epsilon}_b$-polarized radiation into $\hat{\epsilon}_a$-polarized radiation, where $\hat{\epsilon}_x$ and $\hat{\epsilon}_y$ are understood to be *any convenient orthogonal polarization vectors* (linear, circular, or elliptical).

The forward-scattering amplitude f_{ab} now contains a resonant nuclear contribution in addition to the nonresonant electronic contribution,

$$f_{ab} = (f_N)_{ab} + (f_e)_{ab} \ . \tag{3}$$

The electronic scattering is essentially that of an isotropically responding $E1$ oscillator, and to a very good approximation $(f_e)_{ab}$ is diagonal,

$$(f_e)_{ab} = \delta_{ab} f_e \ , \tag{4}$$

where

$$f_e = -(Z+\Delta f')r_0 + i(\sigma_e/4\pi\lambda)$$

as given by Eq. (4) of paper I.[19] The resonant nuclear scattering, on the other hand, corresponds to scattering from a set of well-defined multipole oscillators, and there is generally strong polarization mixing, with $(f_N)_{ab}$ given by[1,2,9]

$$(f_N)_{ab} = \frac{2\lambda_0 P e^{-k^2\langle x^2\rangle}}{2j_0+1} \left[\frac{\Gamma_\gamma}{\Gamma}\right] \sum_{M=-L}^{L} \sum_{m_0=-j_0}^{j_0} C^2(j_0 L j_1; m_0 M)\hat{\epsilon}_a^* \cdot \mathbf{Y}_{LM}^{(\lambda)}(\hat{\mathbf{k}}_0)[\mathbf{Y}_{LM}^{(\lambda)}(\hat{\mathbf{k}}_0)]^* \cdot \hat{\epsilon}_b / [x(m_0 M) - i] \ . \tag{5}$$

Here, Γ_γ is the radiative width, Γ is the total width (radiative, internal conversion, and inhomogeneous broadening),

$$x(m_0 M) = 2[E(j_1, m_0+M) - E(j_0, m_0) - \hbar\omega]/\Gamma \ ,$$

$M = \Delta J_z = m_1 - m_0$, P is the fraction of resonant nuclei, and the notation for the Clebsch-Gordan coefficients is that of Rose.[27] Also in Eq. (5), $\lambda = 0$ or 1 designates the multipole [$(L,1) = EL$ = electric 2^L pole; $(L,0) = ML$ = magnetic 2^L pole], and $\mathbf{Y}_{LM}^{(\lambda)}(\hat{\mathbf{k}}_0)$ is the vector spherical harmonic which gives the polarization of the radiation emitted in the $\hat{\mathbf{k}}_0$ direction by an $L\lambda$ multipole oscillator with $\Delta J_z = M$. In the Appendix the explicit expressions for the $\mathbf{Y}_{LM}^{(\lambda)}$ are given for $E1$, $M1$, and $E2$ transitions. It is assumed in Eq. (5) that the transition is a pure $L\lambda$ multipole transition, that the fast-relaxation limit holds (relaxation times short compared to the Larmor precession time τ), and that the "static effective fields" (**B** and EFG) acting on the nucleus have a common axis of symmetry, $\hat{\mathbf{z}}$, so that the ground and excited nuclear states are states of good J_z. The modifications necessary when the transition is a multipole mixture and when J_z is not con-

served are discussed in Ref. 9, and the modifications necessary when relaxation effects are important are discussed in Refs. 28–31.

From the eigenvalue equation (1), the $\hat{\epsilon}_\eta$ eigenpolarization is

$$\hat{\epsilon}_\eta = K_{(\eta,x)}[\hat{\epsilon}_x + (f_\eta - f_{xx})/f_{xy}\hat{\epsilon}_y], \quad \eta = \mathrm{I,II} \tag{6}$$

where the normalization constant is

$$K_{(\eta,x)} = [1 + |(f_\eta - f_{xx})/f_{xy}|^2]^{-1/2} ,$$

and the coherent elastic forward-scattering amplitude for $\hat{\epsilon}_\eta$ polarization is

$$\begin{aligned} f_\eta &= \hat{\epsilon}_\eta \cdot \tilde{f} \cdot \hat{\epsilon}_\eta \\ &= \tfrac{1}{2}\mathrm{Tr}(\tilde{f}) + (-1)^{(\eta+1)}\{[\tfrac{1}{2}\mathrm{Tr}(\tilde{f})]^2 - \det(\tilde{f})\}^{1/2} \\ &= \tfrac{1}{2}(f_{xx}+f_{yy}) + (-1)^{(\eta+1)}[\tfrac{1}{4}(f_{xx}-f_{yy})^2 + f_{xy}f_{yx}]^{1/2} \\ &= f_e + f_N(\eta) . \end{aligned} \tag{7}$$

Here, $f_N(\eta)$ is just the nuclear contribution to f_η, and f_e is the purely electronic contribution given by Eq. (4). We note that the eigenpolarizations are determined entirely by the nuclear scattering. For the electronic scattering any polarization is an eigenpolarization due to the isotropic response.

The critical reflection of an incident $\hat{\epsilon}_\eta$ eigenpolarization can then be treated as in paper I, giving the reflection amplitude

$$R_\eta(\omega,\phi) = [1-\beta(\eta)]/[1+\beta(\eta)] , \tag{8}$$

where

$$\begin{aligned} \beta(\eta) &= (1 + n\lambda^2 f_\eta/\pi\phi^2)^{1/2} \\ &= [1 - (\phi_c/\phi)^2 + i(\lambda/\phi^2 l_A) + n\lambda^2 f_N(\eta)/\pi\phi^2]^{1/2} . \end{aligned} \tag{9}$$

Because of the optical activity associated with nuclear scattering, the reflectivity depends strongly on the incident polarization.

A. Orthogonal eigenpolarizations

An important point to notice is that $(f_N)_{ab}$, and hence the scattering matrix $\tilde{f}$, is not Hermitian, so the eigenvectors $\hat{\epsilon}_\mathrm{I}, \hat{\epsilon}_\mathrm{II}$ are generally nonorthogonal.[9,25] As discussed in Ref. 9, however, there are three important cases when the eigenpolarizations are orthogonal: (1) If the internal field **B** at the nucleus is perpendicular to $\mathbf{k}_0$, then the eigenpolarizations are *linear*, with $\hat{\epsilon}_y \| \mathbf{B}$, $\hat{\epsilon}_x \| \mathbf{B}\times\mathbf{k}_0$. If **B** is parallel to the surface of the medium and perpendicular to $\mathbf{k}_0$, then the eigenpolarizations are the linear basis $\hat{\epsilon}_x = \hat{\epsilon}_\pi$, $\hat{\epsilon}_y = \hat{\epsilon}_\sigma$. (2) If $\mathbf{B}\|\mathbf{k}_0$, then the eigenpolarizations

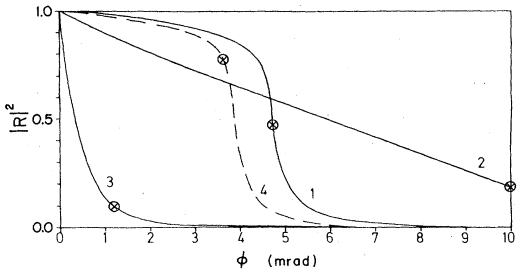

FIG. 1. $|R(\phi,\omega)|^2$ vs ϕ for reflection from resonant ^{57}Fe mirror for different near-resonance frequencies $\Delta/\Gamma = (\hbar\omega - E_{\mathrm{res}})/\Gamma = 12$, 0, -5, and -45 for curves 1–4, respectively. Here we assume a single resonance and use the oscillator strength f_0 appropriate for reflection of $\hat{\epsilon}_{(+1)}$ radiation by the $+\frac{1}{2} \rightarrow +\frac{3}{2}$ transition with $\mathbf{B}\|\mathbf{k}_0$. The crosses indicate the angles $\phi_c^*(\omega)$. The x-ray critical angle is $\phi_c = 3.8$ mrad.

are the right- and left-circularly-polarized bases,

$$\hat{\epsilon}_x = \hat{\epsilon}_{(+1)} = -(1/\sqrt{2})[\hat{\epsilon}_\pi + i\hat{\epsilon}_\sigma] ,$$
$$\hat{\epsilon}_y = \hat{\epsilon}_{(-1)} = (1/\sqrt{2})[\hat{\epsilon}_\pi - i\hat{\epsilon}_\sigma] .$$

(3) Finally, in the limit of no Zeeman splitting the nuclear as well as the electronic scattering responds isotropically, and *any* orthogonal basis serves as an eigenbasis [see Appendix, Eq. (A6)].

Whenever the eigenbases are orthogonal, the reflectivity for incident $\hat{\epsilon}_0$-polarized radiation is then simply

$$|R(\omega,\phi)|^2 = \sum_{\eta=\mathrm{I,II}} |R_\eta|^2 \, |\hat{\epsilon}_0^* \cdot \hat{\epsilon}_\eta|^2 . \tag{10}$$

In Fig. 1 we plot $|R(\omega,\phi)|^2$ versus ϕ for different frequencies about a resonance, and in Fig. 2(a) we give contour plots of $|R(\omega,\phi)|^2$ versus ϕ and ω. Here we consider only a *single* resonance so that $f_N = f_0/(x-i)$ in Eq. (5), $x = 2[\Delta E - \hbar\omega]/\Gamma$, and for f_0 we use the factors appropriate for grazing incidence of right-circular-polarized radiation in near resonance with the $m_0 = +\frac{1}{2} \leftrightarrow m_1 = +\frac{3}{2}$ resonance of ^{57}Fe with $\mathbf{B}\|\mathbf{k}_0$. The factor β in Eq. (8) is now

$$\beta = \left\{ 1 - \phi^{-2} \left[\left[\phi_c^2 - \frac{n\lambda\sigma_0 x}{x^2+1} \right] - i \left[\frac{n\lambda\sigma_0}{x^2+1} + n\lambda\sigma_e \right] \right] \right\}^{1/2} , \tag{11}$$

where $\sigma_0 = 4\pi\lambda f_0$ is the resonance cross section. The nature of the falloff of $|R|^2$ with ϕ now depends on which term is dominant, $n\lambda\sigma_0/(x^2+1)$ or $[\phi_c^2 - n\lambda\sigma_0 x/(x^2+1)]$, and whether the latter term is positive or negative. There is no true critical angle in the resonance region due to the large absorption, but a rough characterization of the curves is given by the "frequency-dependent critical angle"

$$\phi_c^*(\omega) = \max\{[\,|n\lambda\sigma_0 x/(x^2+1) - \phi_c^2|\,]^{1/2}, [n\lambda\sigma_0/(x^2+1)]^{1/2}\} . \tag{12}$$

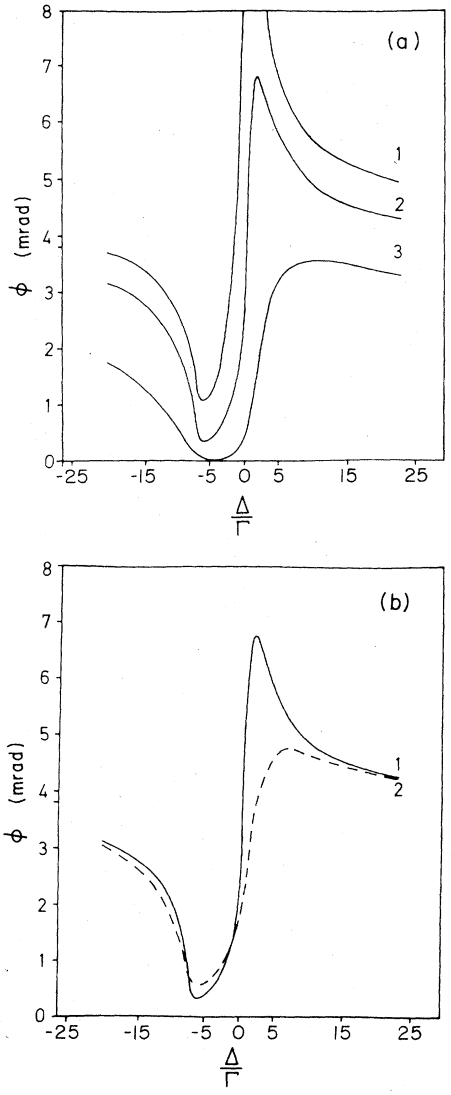

FIG. 2. (a) Contour plots of $|R(\phi,\omega)|^2$ for $|R|^2=0.25$, 0.5, and 0.9 for curves 1—3, respectively. (b) Contour plots for 50% reflection with oscillator strength f_0 (solid line) and with $f_0 \rightarrow \frac{1}{4}f_0$ (dashed line). The critical angle is $\phi_c = 3.8$ mrad.

In Fig. 1 the positions of $\phi_c^*(\omega)$ are indicated by crosses. The region $\phi < \phi_c^*(\omega)$ is a region of strong scattering for a wave of frequency ω. As a function of frequency, $\phi_c^*(\omega)$ maximizes on the high-frequency side of resonance, where the nuclear contribution to the index of refraction interferes constructively with the electronic contribution, and the angular region of strong reflection is much broader than far off resonance. Correspondingly, there is a minimum for $\phi_c^*(\omega)$ on the low-frequency side of resonance, where the nuclear contribution interferes destructively with the electronic contribution, and the angular region of strong scattering is much smaller than far off resonance. In Fig. 2(a), $\phi_c^*(\omega)$ is given approximately by the contour line for 50% reflection.

From Fig. 2(a) it is clear that if the beam is incident below the electronic ϕ_c, then as a function of frequency the reflected intensity will exhibit a sharp *minimum* on the low-frequency side of resonance [where $\phi_c^*(\omega)$ minimizes]. Similarly, if $\phi > \phi_c$, the reflected intensity will have a sharp *maximum* on the high-frequency side of resonance [where $\phi_c^*(\omega)$ maximizes].

B. Oscillator strengths: Polarization dependence

The magnitude of the near-resononance reflectivity depends on the "oscillator strength." In Fig. 2(b) we show the effect of reducing the strength of the resonance: the solid line gives the contour $|R|^2=0.5$ with f_0 given as before, while for the dashed line $f_0' = \frac{1}{4}f_0$. To otain a strong nuclear reflection above ϕ_c, it is clearly necessary to maximize the oscillator strength.

As shown explicitly in Eq. (5), the strength of a resonance for a given transition M depends on several factors: the coupling of the oscillator to the incident polarization, $|\mathbf{Y}_{LM}^{(\lambda)}(\hat{\mathbf{k}}_0)\cdot\hat{\boldsymbol{\epsilon}}_0|^2$; the homogeneous and inhomogeneous broadening, Γ_γ/Γ; the fraction of resonant nuclei, P; and the Mössbauer phonon factor, $\exp(-k^2\langle x^2\rangle)$. The aspect of inhomogeneous broadening is discussed in a later section. Here we consider the polarization response.

For the particular case of an $M1$ transition such as

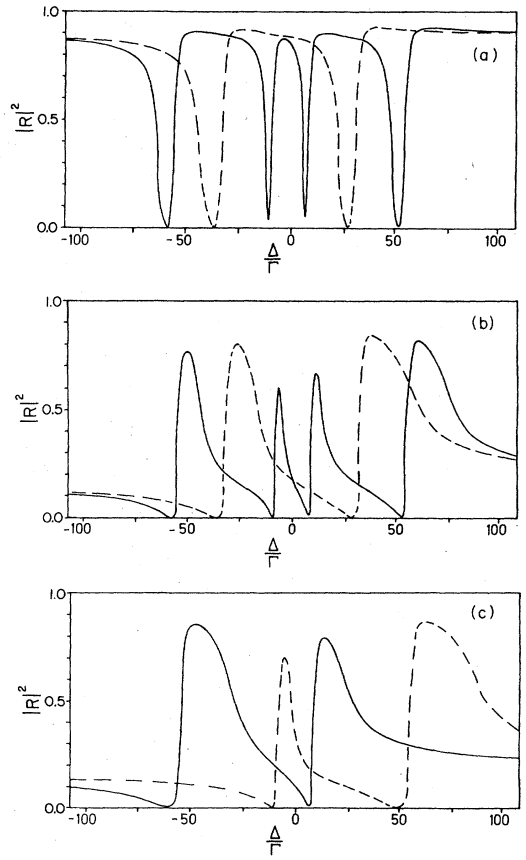

FIG. 3. $|R(\omega,\phi)|^2$ vs ω for reflection from a resonant mirror for (a) $\mathbf{B}\perp\mathbf{k}_0$, $\phi=3.0$ mrad, and (b) $\phi=4.4$ mrad. The solid line gives the response for incident $\hat{\boldsymbol{\epsilon}}_\sigma$, the dashed line for incident $\hat{\boldsymbol{\epsilon}}_\pi$; (c) $\mathbf{B}\|\mathbf{k}_0$, $\phi=4.4$ mrad. The solid line is for incident $\hat{\boldsymbol{\epsilon}}_{(+1)}$, the dashed for incident $\hat{\boldsymbol{\epsilon}}_{(-1)}$.

^{57}Fe, there are three types of oscillators, $M=0,\pm1$. The $M=0$ transitions correspond to linear magnetic dipole oscillators constrained to oscillate along the $\hat{\mathbf{z}}'=\hat{\mathbf{B}}$ axis, where $\mathbf{B}$ is the internal field at the nucleus. The $M=\pm1$ transitions correspond to circular $M1$ oscillators constrained to circulate in the plane perpendicular to $\mathbf{B}$, in a right- or left-hand fashion about the $+\mathbf{B}$ axis. The response to incident radiation then depends on the orientation of the quantization axis $\mathbf{B}$ of the oscillator relative to the incident $\mathbf{k}_0$.

In Figs. 3(a) and 3(b) we plot $|R(\omega,\phi)|^2$ versus ω for grazing-incidence reflection from ^{57}Fe at angles $\phi=3.0$ and 4.4 mrad which lie below and above the electronic critical angle $\phi_c=3.8$ mrad. Here the magnetic field at the nucleus lies in the plane of the film and perpendicular to $\mathbf{k}_0$, so the eigenpolarizations are the linear basis $\hat{\epsilon}_\pi,\hat{\epsilon}_\sigma$. The solid lines give the response to incident $\hat{\epsilon}_\sigma$. The two $M=0$ transitions couple only to $\hat{\epsilon}_\pi$ radiation, and the four $M=\pm1$ transitions couple only to $\hat{\epsilon}_\sigma$ radiation. The strongest polarization coupling is that of the $\hat{\epsilon}_\pi$ polarization to the linear $M=0$ oscillators [$|\hat{\epsilon}_\pi\cdot\hat{\mathbf{Y}}^{(0)}_{10}(\hat{\mathbf{k}}_0)|^2=1$, while $|\hat{\epsilon}_\sigma\cdot\hat{\mathbf{Y}}^{(0)}_{1\pm1}(\hat{\mathbf{k}}_0)|^2=\frac{1}{2}$]. The Clebsch-Gordan coefficients are $C^2=\frac{2}{3}$ for the two $M=0$ transitions, $C^2=1$ or $\frac{1}{3}$ for the two $M=+1$ transitions (the strongest is the $+\frac{1}{2}\rightarrow+\frac{3}{2}$ transition), and similarly $C^2=1$ or $\frac{1}{3}$ for the two $M=-1$ transitions. For this geometry, the strongest oscillator strengths then occur for the $M=0$ transitions ($C^2|\hat{\epsilon}_\pi\cdot\hat{\mathbf{Y}}^{(0)}_{10}|^2=\frac{2}{3}$, while $C^2|\hat{\epsilon}_\sigma\cdot\hat{\mathbf{Y}}^{(0)}_{1\pm1}|^2=\frac{1}{2}$ or $\frac{1}{6}$), and we see in Fig. 3(b) that the strongest effects (higher peak reflectivities and broader widths) occur near these resonances.

As expected, for $\phi<\phi_c$, a sharp minimum occurs on the low-frequency side of each resonance, while for $\phi>\phi_c$ a sharp maximum occurs on the high-frequency side of each resonance. Thus for $\phi>\phi_c$ a strong nuclear reflection can be obtained, but the "signal-to-noise" ratio is still very limited, $|R|^2_{\rm res}/|R|^2_{\rm nonres}\approx4$.

In Fig. 3(c) we give the corresponding results for $\phi=4.4\times10^{-3}$ rad with $\mathbf{B}||\mathbf{k}_0$, for which the eigenpolarizations are the circular basis $\hat{\epsilon}_{(\pm1)}$. Now the solid line gives the response for $\hat{\epsilon}_{(+1)}$ radiation, and the dashed line for $\hat{\epsilon}_{(-1)}$ radiation. In this geometry the $M=+1$ transitions couple only to the $\hat{\epsilon}_{(+1)}$ radiation, the $M=-1$ transitions couple only to $\hat{\epsilon}_{(-1)}$ radiation, and the $M=0$ transitions are unexcited. The polarization coupling is now maximal, $|\hat{\epsilon}^*_{(\pm1)}\cdot\hat{\mathbf{Y}}^{(0)}_{1\pm1}|^2=1$ and the oscillator strengths are $C^2|\hat{\epsilon}_{(\pm1)}\cdot\hat{\mathbf{Y}}^{(0)}_{1\pm1}|^2=1$ or $\frac{1}{3}$. We note that in this geometry the oscillator strengths for the two strong $M=\pm1$ transitions ($\pm\frac{1}{2}\leftrightarrow\pm\frac{3}{2}$, for which $C^2=1$) are stronger than the oscillator strengths of the $M=0$ transitions with $\mathbf{B}\perp\mathbf{k}_0$, and, in fact, this geometry gives the maximum possible oscillator strength in the case of Zeeman splitting. The only possible stronger coupling is for the unsplit case, for which the oscillator strength is increased from 1 to $\frac{4}{3}$.

C. Nonorthogonal eigenbasis

The eigenbases $\hat{\epsilon}_{\rm I},\hat{\epsilon}_{\rm II}$ are generally nonorthogonal due to the non-Hermitian nature of the scattering matrix $\tilde{f}$, and the expressions for the reflectivities are then modified.

Expressing the incident wave as

$$\mathbf{A}_0=a_{0x}\hat{\epsilon}_x+a_{0y}\hat{\epsilon}_y=\begin{bmatrix}a_{0x}\\a_{0y}\end{bmatrix}, \tag{13}$$

the scattered-wave amplitude is then

$$\mathbf{A}_s=\tilde{R}\,\mathbf{A}_0\,, \tag{14}$$

where the reflection matrix is given by[9,10]

$$\tilde{R}=\begin{bmatrix}R_{xx}&R_{xy}\\R_{yx}&R_{yy}\end{bmatrix}=\begin{bmatrix}\frac{1}{2}\left[R_{(+)}+R_{(-)}\left[\frac{f_{xx}-f_{yy}}{f_{\rm I}-f_{\rm II}}\right]\right] & \left[\frac{f_{xy}}{f_{\rm I}-f_{\rm II}}\right]R_{(-)}\\ \left[\frac{f_{yx}}{f_{\rm I}-f_{\rm II}}\right]R_{(-)} & \frac{1}{2}\left[R_{(+)}-R_{(-)}\left[\frac{f_{xx}-f_{yy}}{f_{\rm I}-f_{\rm II}}\right]\right]\end{bmatrix}, \tag{15}$$

where

$$R_{(\pm)}=R_{\rm I}\pm R_{\rm II}\,, \tag{16}$$

and where R_η and f_η, $\eta=$I,II, are given by Eqs. (7) and (8). We note again that here $\hat{\epsilon}_x$ and $\hat{\epsilon}_y$ are *any* convenient orthogonal basis vectors—linear, circular, or elliptical.

Equations (14) and (15) give the general expression for the reflected wave and are valid for the special cases of orthogonal eigenbases as well as the more general nonorthogonal case. In the special orthogonal cases, *if* the eigenbases $\hat{\epsilon}_{\rm I},\hat{\epsilon}_{\rm II}$ are used as the basis vectors $\hat{\epsilon}_x,\hat{\epsilon}_y$, then $f_{xx}=f_{\rm I}$, $f_{yy}=f_{\rm II}$, $f_{xy}=f_{yx}=0$, and $\tilde{R}$ diagonalizes. More generally, the off-diagonal matrix element R_{xy} (R_{yx}) accounts for the orthogonal scattering $\hat{\epsilon}_y\rightarrow\hat{\epsilon}_x$ ($\hat{\epsilon}_x\rightarrow\hat{\epsilon}_y$), which is generally very strong for the resonant medium (for example, if $\mathbf{B}||\mathbf{k}_0$, then the scattered radiation will be circularly polarized even for incident linear polarization).

III. RESONANT REFLECTION FROM A LAYERED MEDIUM

We now consider grazing-incidence reflection of resonance radiation from a layered medium in which one or

more of the films or substrate is resonant.

A. Single film

For a substrate coated with a single film, either the substrate or the film is resonant. For the nonresonant medium, *any* polarization is an eigenpolarization since only electronic scattering is involved. Therefore the eigenpolarizations for the *compound* system are determined by the *resonant medium.* The eigenpolarizations $\hat{\epsilon}_\eta$ are then given by Eq. (6), with all scattering amplitudes referring to the *resonant medium.*

The reflection amplitude for the compound system for incident $\hat{\epsilon}_\eta$ eigenpolarization is then given by Eq. (9) of paper I,

$$R_\eta(\omega,\phi)=\frac{R_{01}(\eta)+R_{12}(\eta)e^{2ig_1(\eta)l_1}}{1+R_{01}(\eta)R_{12}(\eta)e^{2ig_1(\eta)l_1}}\ , \tag{17}$$

where, as before,

$$R_{01}(\eta)=(1-\beta_1)/(1+\beta_1)\ ,$$

$$R_{12}(\eta)=(\beta_1-\beta_2)/(\beta_1+\beta_2)\ ,$$

and $g_1(\eta)=k\phi\beta_1$, but now either β_1 or β_2 contains the resonant nuclear contribution $n\lambda^2 f_N(\eta)/\pi\phi^2$ as given in Eq. (9).

For incident $\hat{\epsilon}_0$, the reflected amplitude is then determined by Eq. (14), with the scattering amplitudes f_{xx}, f_{yy}, f_{xy}, f_{yx}, $f_{\rm I}$, and $f_{\rm II}$ being those of the *resonant medium,* while the eigenpolarization reflection amplitudes $R_{\rm I},R_{\rm II}$, which determine $R_{(\pm)}$, are now the compound reflection amplitudes given by Eq. (17). For the special cases of orthogonal polarizations, the reflectivity is also given by Eq. (10) with the compound reflectivities $R_{\rm I},R_{\rm II}$.

B. Multilayer films

For the more general case of a substrate coated with multiple films, then one or more of the film layers or substrate can be resonant.

If the resonant medium occurs more than once, then we will assume that the internal fields have the same orientation in all the resonant layers. With this simplifying assumption, the eigenpolarizations $\hat{\epsilon}_\eta$ will then be the same for each resonant layer, as will be the eigenpolarizations for the compound medium.

For such a multilayered medium, the expressions (12) and (13) of paper I are appropriate, modified for the optical activity of the resonant reflection. For two films on a substrate, the reflection amplitude for $\hat{\epsilon}_\eta$ eigenpolarization is given by

$$R_\eta(\omega,\phi)=\frac{R_{01}(\eta)+R_{12}^{\dagger}(\eta)e^{2ig_1(\eta)l_1}}{1+R_{01}(\eta)R_{12}^{\dagger}(\eta)e^{2ig_1(\eta)l_1}}\ , \tag{18}$$

where $R_{12}^{\dagger}$ is the *compound* reflection amplitude at the 1-2 interface,

$$R_{12}^{\dagger}(\eta)=\frac{R_{12}(\eta)+R_{23}(\eta)e^{2ig_2(\eta)l_2}}{1+R_{12}(\eta)R_{23}(\eta)e^{2ig_2(\eta)l_2}}\ , \tag{19}$$

and here

$$R_{23}(\eta)=(\beta_2-\beta_3)/(\beta_2+\beta_3)$$

is the reflection amplitude at the substrate interface. For more than two films, R_{23} is replaced by the compound reflectivity $R_{23}^{\dagger}$ in Eq. (19) and the iteration is continued.

IV. PURE NUCLEAR REFLECTIONS

Very pure coherent resonant scattering can now be obtained by using a grazing-incidence antireflection (GIAR) film in which one or more of the layers or substrate contain the resonant nuclei. Off-resonance radiation is then strongly suppressed by destructive interference, while near resonance the sensitive phase- and impedance-matching conditions of the antireflection film are destroyed, and very strong resonant reflection can occur.

A. Resonant mirror coated with a nonresonant λ/4 GIAR film

As an illustrative example, we consider a resonant ^{57}Fe mirror coated with an impedance-matched quarter-wave film of Te.

As discussed in paper I, the optimum film thickness for Te is then $l_1\approx 76$ Å, and the maximum suppression is for $\phi_0\approx 4.4$ mrad. The nonresonant reflectivity, averaged over a 0.25-mrad beam divergence and a thickness variation of $\pm 2.5\%$ l_1, is then $|R|^2_{\rm nonres}\approx 9.4\times 10^{-4}$. In Figs. 4(a) and 4(b) we plot the near-resonant reflectivity versus ω for $\phi_0=4.4$ mrad for different orientations of **B** and different incident polarizations. In Fig. 4(a) we take $\mathbf{B}\perp\mathbf{k}_0$ as in Fig. 3(b), and again the solid line gives the response to $\hat{\epsilon}_\sigma$ polarization and the dashed line that to $\hat{\epsilon}_\pi$ polarization. In Fig. 4(b) we take $\mathbf{B}\|\mathbf{k}_0$, and the solid line gives

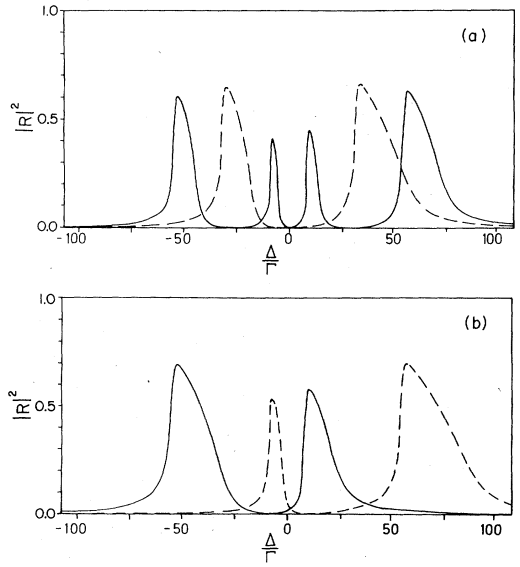

FIG. 4. $|R(\omega,\phi)|^2$ vs ω for reflection from a resonant ^{57}Fe mirror coated with a 76-Å film of Te, with $\phi=4.4$ mrad for (a) $\mathbf{B}\perp\mathbf{k}_0$, incident $\hat{\epsilon}_\sigma$ (solid line) and incident $\hat{\epsilon}_\pi$ (dashed line); (b) $\mathbf{B}\|\mathbf{k}_0$, incident $\hat{\epsilon}_{(+1)}$ (solid line) and incident $\hat{\epsilon}_{(-1)}$ (dashed line).

the response to $\hat{\epsilon}_{(+1)}$ radiation and the dashed that to $\hat{\epsilon}_{(-1)}$ radiation.

Comparing the results of Figs. 4(a) and 4(b) with the corresponding results of Figs. 3(a) and 3(b) obtained from uncoated ^{57}Fe, we see the peak reflectivities and widths are reduced about 18% due to the removal of the electronic scattering and due to photoabsorption in the Te film. Still there are very strong peak reflectivities, ≈ 0.7, and strongly broadened resonance widths, $\approx 25\Gamma$, and for the strongest (± 1) oscillators of Fig. 4 the peak resonant to nonresonant signal-to-noise ratio is $|R|^2_{\rm res}/|R|^2_{\rm nonres} \approx 745$. The strong resonance broadening is due to refraction-augmented "enhancement" as discussed below. Comparing the results of Figs. 4(a) and 4(b), the stronger response for $\mathbf{B}||\mathbf{k}_0$ is again due to the stronger oscillator strengths for this geometry.

In Table I we give the peak reflectivities $|R|^2_{\rm res}$ and resonance widths $\Gamma_{\rm eff}$ (for $\mathbf{B}||\mathbf{k}_0$ and incident $\hat{\epsilon}_{(+1)}$ radiation) and the "signal-to-noise" ratios $|R|^2_{\rm res}/|R|^2_{\rm nonres}$ for various $\lambda/4$ GIAR films on ^{57}Fe, with ϕ_0 and l_1 taken as the optimal parameters which minimize the electronic scattering (see Table III of paper I). We note, in particular, that the resonant reflectivity and widths $\Gamma_{\rm eff}$ can be increased by picking a film which gives minimum electronic reflectivity at $\phi_{\rm min} \approx \phi_c({\rm Fe}) = 3.8\times 10^{-3}$ rad. For example, for a Zr film the optimal parameters are $l_1 \approx 96$ Å and $\phi_{\rm min} \approx 4.2\times 10^{-3}$ rad. In this case the peak nuclear reflectivity is $|R|^2_{\rm res} \approx 0.76$ and $\Gamma_{\rm eff} \approx 25$. However, because of the more rapid variation of R_{12} as $\phi \to \phi_c$, the nonresonant reflectivity is now increased to $|R|^2_{\rm nonres} \approx 4.7\times 10^{-3}$, and the signal-to-noise ratio is, in fact, decreased from the Te-coating case.

B. Refraction-augmented enhancement effect

The strong broadening of the resonance line which occurs when $\phi_0 \approx \phi_c$ is due to the "enhancement effect," augmented by refraction.

In Fig. 5(a) we plot the reflectivity $|R|^2$ versus ω in the region of the strong $M=+1$ transition ($+\frac{1}{2} \to +\frac{3}{2}$) for $\hat{\epsilon}_{(+1)}$ radiation incident at $\phi = 4.4$ mrad on a Te-coated resonant mirror with $\mathbf{B}||\mathbf{k}_0$ (solid line), and we also give the corresponding curve for reflection from a hypothetical "pure nuclear mirror" with the electronic system removed (dashed line).

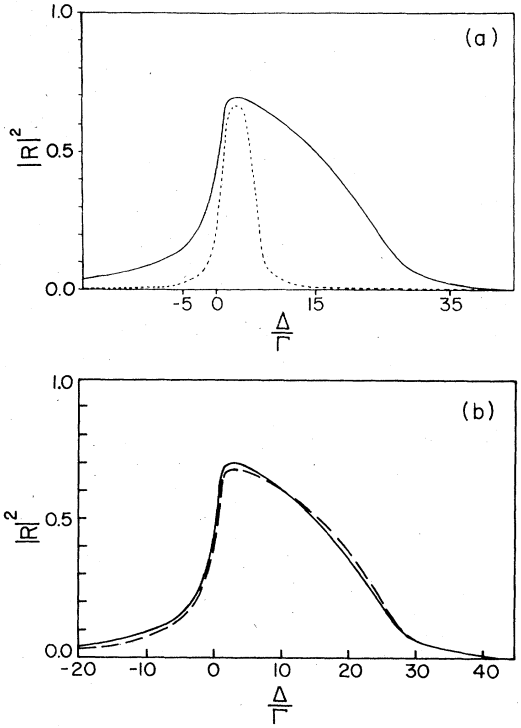

FIG. 5. The solid lines give $|R(\omega,\phi)|^2$ vs ω for reflection of $\hat{\epsilon}_{(+1)}$ radiation by $+\frac{1}{2} \to +\frac{3}{2}$ transition of ^{57}Fe mirror coated with a 76-Å film of Te, and with $\phi = 4.4$ mrad. In (a) the dashed line gives the corresponding reflection from a pure nuclear mirror (i.e., with the electronic Thomson scattering and photoabsorption set equal to zero). In (b) the dashed line gives the pure nuclear reflection as given by Eq. (23).

The important feature to note here is the width of the response: for the "pure nuclear mirror" the width at half maximum is enhanced to $\approx 5\Gamma$, while for the antireflection coated mirror the width is further augmented to $\approx 20\Gamma$.

The 5Γ broadening of the hypothetical pure nuclear mirror is a consequence of the "enhancement effect" first pointed out by Trammell:[1,9] For waves incident near

TABLE I. Peak resonant reflectivities $|R|^2_{\rm res}$, effective widths $\Gamma_{\rm eff}$, and signal-to-noise ratios $|R|^2_{\rm res}/|R|^2_{\rm nonres}$ for several $\lambda/4$ antireflection films on ^{57}Fe. The results are for the $+\frac{1}{2} \to +\frac{3}{2}$ transition reflecting $\hat{\epsilon}_{(+1)}$ radiation with $\mathbf{B}||\mathbf{k}_0$, and the off-resonance response has been averaged over an incident-beam spread of 0.25 mrad and over a long-range film-thickness variation of $l_1 \pm 0.025 l_1$.

	ϕ_0 (mrad)	l_1 (Å)	$\lvert R\rvert^2_{\rm res}$	$\Gamma_{\rm eff}$	$\lvert R\rvert^2_{\rm res}/\lvert R\rvert^2_{\rm nonres}$
$_{22}$Ti	6.02	42	0.57	5Γ	2.38×10^4
$_{34}$Se	6.03	40	0.53	5Γ	2.52×10^4
$_{32}$Ge	4.57	65	0.61	15Γ	1.65×10^3
$_{52}$Te	4.38	76	0.70	20Γ	745
$_{31}$Ga	4.21	85	0.59	22Γ	219
$_{23}$V	4.19	93	0.71	24Γ	203
$_{51}$Sb	4.15	97	0.66	24Γ	127
$_{58}$Ce	4.12	98	0.59	23Γ	82
$_{40}$Zr	4.17	96	0.76	25Γ	162

Bragg or grazing incidence (which is a special $\phi_B=0$ "Bragg" condition) on a resonant medium, there is a broadened width of the frequency response due to coherent reemission into the reflection channel, and, correspondingly, the time response for coherent scattering is sped up relative to the natural lifetime for incoherent decay and internal conversion absorption. This gives an enhancement of the coherent scattering and consequent suppression of the incoherent processes.

For a true *Bragg* reflection, the detailed mechanism of enhancement depends on the deviation $\delta\phi$ from exact Bragg condition.[32] At exact Bragg ($\delta\phi=0$), a simple semistationary collective state is created which decays as $\exp[-(\Gamma+\Gamma_c)t]$, where the coherence width Γ_c is proportional to the number of crystal planes. On the wings of the Bragg reflection the broadening is more kinematical in nature: Qualitatively, the broadening occurs here because off-resonance radiation ω, which is scattered more weakly than resonance radiation ω_0 by each plane layer, simply penetrates deeper into the crystal, scattering from a larger number of layers and resulting in a strong Bragg reflection of frequency ω. However, for a given $\delta\phi$ off Bragg, only radiation from M layers, $M\lesssim\lambda\!\!\!^{-}/(d\cos\phi_0\,\delta\phi)$ can be kept in phase, and for deeper penetration destructive interference sets in. Thus beyond a certain frequency deviation from resonance, determined by the angular deviation off Bragg and the strength of the nuclear scattering, the penetration depth becomes too deep and there is no strong reflection. The resulting spread of frequencies reflected has a width

$$\Gamma_{\rm eff}(\delta\phi)\approx\lambda\!\!\!^{-}n\sigma_0\Gamma/\sin(2\phi_0)\delta\phi\ .$$

Although here we no longer have the creation of a simple semistationary collective state, still the broadened frequency response leads to a speeding up of coherent decay, which prevents any appreciable incoherent decay.

For grazing incidence, which is on the wing of the exact "Bragg" condition $\phi_B=0$, the broadening is also kinematical in nature and similar arguments can be constructed. However, here it is easiest to think in terms of the frequency-dependent critical angle: for a wave incident at ϕ on a pure nuclear mirror, there will be strong reflection over those frequencies ω for which

$$\phi_c(\omega)=[-n\lambda\!\!\!^{-}\sigma_0 x/(x^2+1)]^{1/2}>\phi\ ,$$

which gives

$$\Gamma_{\rm eff}(\phi)\approx\lambda\!\!\!^{-}n\sigma_0\Gamma/2\phi^2\ . \tag{20}$$

Again the broadened response leads to sped-up decay into the reflection channel, with consequent suppression of the incoherent processes.

For the pure nuclear reflection considered in Fig. 5(a), $\sigma_0=1.5\times10^{-18}$ cm^2, $n=8.5\times10^{22}$ cm^{-3}, and the estimate, Eq. (20), gives $\Gamma_{\rm eff}(\phi)\approx4.7\Gamma$, in good agreement with the calculated value.

The additional augmentation of the width from $5\Gamma\rightarrow20\Gamma$ for the antireflection coated mirror is an index-of-refraction effect. A qualitative argument is the following: Consider an ^{57}Fe mirror coated with an ^{56}Fe film of thickness $l(^{56}\text{Fe})\rightarrow0$, which, in turn, is coated with an impedance-matched $\lambda/4$ film is indicated in Fig. 6. The reflections R_{01} and R_{12} are purely electronic, and because of the impedance matching the two reflected waves completely cancel. The net reflected wave is then only that arising from the ^{56}Fe-^{57}Fe interface, which is entirely due to the nuclear contribution to the index of refraction. Thus the reflected wave is a pure nuclear reflection, but because of refraction within the ^{56}Fe medium, the effective angle of incidence on the resonant ^{57}Fe medium is

$$\phi'=\phi\{1-[\phi_c(\text{Fe})/\phi]^2\}^{1/2}\ . \tag{21}$$

For Fe coated with Te, then $\phi=4.4$ mrad, while $\phi_c(\text{Fe})=3.8$ mrad, so the effective angle of incidence is decreased to only 2.2 mrad. This decrease in the effective incidence angle then causes an increase of the enhanced width $\Gamma_{\rm eff}$ of Eq. (20) by a factor $\{1-[\phi_c(\text{Fe})/\phi]^2\}^{-1}$, so for the coated mirror the effective width is

$$\Gamma_{\rm eff}(\phi)\approx\lambda\!\!\!^{-}n\sigma_0\Gamma/2[\phi^2-\phi_c(\text{Fe})^2]\ . \tag{22}$$

Thus for Fe coated with Te, refraction should augment the widths by a factor of $\approx4x$, in good agreement with the results shown in Fig. 5(a).

More explicitly, since the reflected wave is just that arising from the ^{56}Fe-^{57}Fe interface when the antireflection condition holds, then the reflection amplitude is given, to a good approximation, by the simple expression

$$R_\eta(\phi,\omega)\approx\{[1-\beta_N(\eta)]/[1+\beta_N(\eta)]\}e^{2ig_1l_1}\ , \tag{23}$$

where β_N is the ratio $\beta(^{57}\text{Fe})/\beta(^{56}\text{Fe})$,[33]

$$\beta_N(\eta)=\{1+n\lambda^2f_N(\eta)/\pi[\phi^2-\phi_c(2)^2+i\lambda\!\!\!^{-}n\sigma_e]\}^{1/2}\ , \tag{24}$$

and here $f_N(\eta)$ is the nuclear forward-scattering amplitude for $\hat{\epsilon}_\eta$ eigenpolarization. These results show that the reflection is a pure nuclear reflection, with a nuclear oscillator strength increased by refraction,

$$f_N\rightarrow f_N/[1-(\phi_c/\phi)^2+i\lambda\!\!\!^{-}n\sigma_e/\phi^2]\ , \tag{25}$$

where ϕ_c is the electronic critical angle of the resonant medium. For Fe coated with Te, the effective oscillator strengths are increased by a factor of $\approx4x$.

The effect of photoabsorption in the resonant medium, which enters through the $in\lambda\!\!\!^{-}\sigma_e$ term in Eq. (24), is to decrease the maximum reflectivity and to induce the frequency asymmetry apparent in Fig. 5(a).

In Fig. 5(b) the dashed line gives $|R|^2$ as given by Eq.

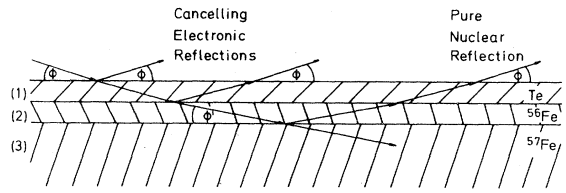

FIG. 6. Schematic of reflection from ^{57}Fe mirror coated with an ^{56}Fe film, which, in turn, is coated with an impedance-matched quarter-wave film of Te.

(23), while the solid line gives the exact response calculated from Eq. (17). The deviations from the exact solid line are due to higher-order multiple-reflection corrections.

C. Inhomogeneous broadening

An important factor which affects the oscillator strength is the inhomogeneous broadening. As given by Eq. (5), the resonant amplitude is proportional to Γ_γ/Γ, where $\Gamma=(1+a)(1+\alpha)\Gamma_\gamma$. Here, a is the coefficient for inhomogeneous broadening, and α is the internal conversion coefficient. Thus strong inhomogeneous broadening will significantly reduce the coherent oscillator strengths.

In the preceding sections, we assumed no inhomogeneous broadening, i.e., $a=0$. However, in the grazing-incidence experiments of Cambell and Bernstein,[4] the effective width seemed to be broadened to about 4Γ (i.e., $a=3$). In this case all oscillator strengths are reduced by $\frac{1}{4}$, which reduces the maximum reflectivities. Thus it is important to try to minimize the amount of inhomogeneous broadening.

The origin of this strong broadening is not entirely clear, but may be due to surface effects, such as nonuniform magnetization near the surface, or surface isomer shifts.

If surface effects are important, then it might be possible to decrease this broadening by coating the ^{57}Fe surface with a film of ^{56}Fe, which, in turn, is coated by the impedance-matched film as shown in Fig. 6. The purpose of the ^{56}Fe is to remove the ^{57}Fe from the surface of the iron. For a Te film, the optimum angle is $\phi\approx 4.4\times 10^{-3}$ rad. The penetration depth in Fe at this angle is $l_\perp\approx 430$ Å, so a ≈ 20-Å coat of ^{56}Fe will still allow most of the radiation through to the ^{57}Fe. Since the electron densities of ^{56}Fe and ^{57}Fe should be equal, there is no additional nonresonant reflection at the ^{56}Fe-^{57}Fe interface, but the resonant radiation will be reflected.

D. Alternate thin-film techniques

In the preceding sections we have shown that pure nuclear reflections can be obtained by coating a resonant mirror with an impedance-matched $\lambda/4$ antireflection film.

Of course, many possible variations of this idea can be obtained by using resonant films or substrates in conjunction with the general theory of grazing-incidence antireflection films developed in papers I and II. The response can, in fact, be tailored to give narrow resonance widths $\Delta\omega\approx\Gamma$ and corresponding delayed scattering times to optimize time filtering, or at the other extreme, to produce filters of very broad width with $\Delta\omega\approx 100\Gamma$, which would be ideal for producing a high-resolution x-ray source. Also, these ideas can be applied to a number of different Mössbauer isotopes.

A systematic investigation of alternate thin-film techniques for producing pure nuclear reflections will be given in a following paper,[22] and here we only briefly mention a few of our current findings.

1. *Broadband resonance filters*

As discussed in paper I, photoabsorption creates a new set of damping stabilized antireflection solutions, with the antireflection minimum occurring very near the critical angle of the upper (lower-density) film. For this case, the minimum is produced by a delicate phase cancellation between two very strong reflections from the upper and lower interfaces. Damping-stabilized minima have proven relatively easy to find experimentally, with minimum reflectivities, typically ≈ 0.05.

By taking a resonant-damping-stabilized GIAR film on a high-density backing, e.g., ^{57}Fe on Ag or ^{57}Fe on Pd, the sensitive conditions for phase cancellation are altered near resonance, leading to very strong resonant reflectivities $\simeq 90\%$ over a very broad frequency half-width $\Delta\omega\simeq(50-100)\Gamma$. Such broadband resonant mirrors would appear ideal for producing high-resolution x-ray sources with $\Delta\omega\simeq 10^{-6}$ eV.

2. *Resonant multilayer techniques*

Various multilayer techniques for antireflection films are discussed in paper II which can be used with resonant films to produce pure nuclear reflections.

One simple technique involves layered ultrathin films of ^{57}Fe and ^{56}Fe, separated by a low-density quarter-wave film—e.g., 15 Å ^{57}Fe—64 Å Be—17 Å ^{56}Fe—Si. For $\phi_0\simeq\phi_c(\mathrm{Fe})=3.8$ mrad, for which the 64-Å Be film is a $\lambda/4$ film, there is strong destructive interference between the Fe layers for nonresonant radiation, with reflectivity $\approx 10^{-4}$, but for resonance radiation the upper ^{57}Fe film is already "thick" due to the strong resonance scattering and absorption, leading to strong specular reflection of the resonance radiation with a reflectivity $\simeq 50\%$ and half-width $\simeq 10\Gamma$.

More generally, for multilayer resonant GIAR mirrors one can use "thickness tuning" to set the operating angle ϕ_0 to systematically vary the resonance response. Ideally, the resonant film should be the top layer, or only coated with films with low photoabsorption cross sections to avoid absorption loses. If the parameters are chosen so that $\phi_0\simeq\phi_c(\mathrm{Fe})$, and if the Fe film is coated on higher-density films, then the response will be similar to the enhanced broadband response of the resonant-damping-stabilized film discussed above. On the other hand, if ϕ_0 is chosen to be well above $\phi_c(\mathrm{Fe})$, then a narrow resonance response will be obtained.

3. *Resonant superlattice GIAR films*

An immediate extension of the layered ^{57}Fe-^{56}Fe ultrathin films discussed above is to increase the number of paired layers to give a resonant superlattice. This would allow the operating angle ϕ_0 to be increased from, say, $\phi_0\approx 5$ mrad up to 10 or 20 mrad. At larger ϕ_0 ($\gtrsim 10$ mrad) the reflection at each interface becomes very weak, but the increased superlattice periodicity builds up a strong total resonant reflection when constructive interference holds, while simultaneously minimizing the nonresonant reflectivity. By increasing ϕ_0, the required size of the mirrors ($\propto 1/\phi_0$) is decreased, and also the noise ef-

fects of coherent small-angle scattering can be decreased.[34] On the other hand, the peak reflectivities for such a superlattice mirror are somewhat reduced, and the resonance widths are only a few Γ.

As a particular example, a 3 Å ^{57}Fe—17 Å Be—3 Å ^{56}Fe—$\cdots$ superlattice mirror has a nonresonant interference minimum of $R\simeq 4\times 10^{-4}$ at $\phi_0=11$ mrad, and a resonant maximum reflectivity of $R\simeq 0.6$ with a resonance width $\Delta\omega\simeq 6\Gamma$. About 25 paired layers are required to saturate the resonance response.

A somewhat less efficient, but probably more easily fabricated, superlattice mirror would be produced by dispensing with the low-density intermediate quarter-wave film and simply using alternating ^{57}Fe-^{56}Fe layers. For this case, when a quarter-wave condition holds, there will be constructive interference for resonant reflections from adjacent interfaces. However, there is no simultaneous nonresonant interference minimum since, for the nonresonant radiation, there is only an index-of-refraction change at the upper interface. A 20 Å ^{57}Fe—20 Å ^{56}Fe—$\cdots$ superlattice mirror has a nonresonant reflectivity of $R_{\rm nonres}\approx 1\times 10^{-3}$ at $\phi_0=12$ mrad, and a resonant reflectivity of $R_{\rm res}\approx 0.5$ with $\Delta\omega\approx 5\Gamma$, while a 10 Å ^{57}Fe—10 Å ^{56}Fe—$\cdots$ superlattice mirror has $R_{\rm nonres}\approx 6\times 10^{-5}$ and $R_{\rm res}\approx 0.4$ with $\Delta\omega\approx 4\Gamma$ at $\phi_0=22$ mrad.

4. *Application to other resonances*

The ideas of thin-film resonant mirrors can also be applied to other low-energy Mössbauer transitions. In particular, we are finding that very efficient resonant mirror systems can be obtained for the 23.9-keV ^{119}Sn transition, the 25.7-keV ^{161}Dy transition, and the 21.6-keV ^{151}Eu transition.

ACKNOWLEDGMENTS

This work was partially supported by grants from the National Science Foundation (No. DMR-80-15706) and the Deutsche Forschungsgemeinschaft and the Bundesministerium für Forschung und Technologie (No. 05269GU), Federal Republic of Germany.

APPENDIX

For reference we summarize here the explicit forms of the vector spherical harmonics $\mathbf{Y}^{\lambda}_{\rm LM}$ for $E1$, $M1$, and $E2$ transitions: For an $E1$ transition ($L=1$, $\lambda=1$)

$$\mathbf{Y}^{(1)}_{10}=-(3/8\pi)^{1/2}(\sin\theta)\hat{\mathbf{e}}_\theta\ ,$$
$$\mathbf{Y}^{(1)}_{1\pm1}=(3/16\pi)^{1/2}e^{\pm i\phi}[\mp(\cos\theta)\hat{\mathbf{e}}_\theta-i\hat{\mathbf{e}}_\phi]\ . \tag{A1}$$

Here, $\hat{\mathbf{e}}_\theta$ and $\hat{\mathbf{e}}_\phi$ are the usual spherical polar unit vectors, and θ and ϕ are the polar and axial angles specifying the photon direction $\mathbf{k}$, with the z axis coinciding with the quantization axis determined by the direction of the internal field at the nucleus. For an $M1$ transition ($L=1$, $\lambda=0$) the spherical harmonics are

$$\mathbf{Y}^{(0)}_{10}=i(3/8\pi)^{1/2}(\sin\theta)\hat{\mathbf{e}}_\phi\ ,$$
$$\mathbf{Y}^{(0)}_{1\pm1}=(3/16\pi)^{1/2}e^{\pm i\phi}[\hat{\mathbf{e}}_\theta\pm i(\cos\theta)\hat{\mathbf{e}}_\phi]\ , \tag{A2}$$

and for an $E2$ transition ($L=2$, $\lambda=1$),

$$\mathbf{Y}^{(1)}_{20}=-(15/32\pi)^{1/2}\sin(2\theta)\hat{\mathbf{e}}_\theta\ ,$$
$$\mathbf{Y}^{(1)}_{2\pm1}=(5/16\pi)^{1/2}e^{\pm i\phi}[\mp\cos(2\theta)\hat{\mathbf{e}}_\theta-i(\cos\theta)\hat{\mathbf{e}}_\phi]\ ,$$
$$\mathbf{Y}_{2\pm2}=(5/16\pi)^{1/2}e^{\pm i2\phi}[\tfrac{1}{2}\sin(2\theta)\hat{\mathbf{e}}_\theta\mp i(\sin\theta)\hat{\mathbf{e}}_\phi]\ . \tag{A3}$$

The relation of the $\mathbf{Y}^{(\lambda)}_{LM}$ to the rotation matrices $\mathscr{D}$ and the circularly-polarized basis

$$\hat{\boldsymbol{\epsilon}}_{(\pm1)}(\hat{\mathbf{k}})=\mp1/\sqrt{2}(\hat{\mathbf{e}}_\theta\pm i\hat{\mathbf{e}}_\phi)$$

is

$$(8\pi/2L+1)^{1/2}\mathbf{Y}^{(\lambda)}_{LM}(\hat{\mathbf{k}})=\hat{\boldsymbol{\epsilon}}_{(+1)}\mathscr{D}^{(L)}_{1M}(\hat{\mathbf{k}},\hat{\mathbf{z}})+(-1)^{(\lambda+1)}\hat{\boldsymbol{\epsilon}}_{(-1)}\mathscr{D}^{(L)}_{-1M}(\hat{\mathbf{k}},\hat{\mathbf{z}})\ , \tag{A4}$$

and the relevant product in Eq. (5) is

$$\hat{\boldsymbol{\epsilon}}^{*}_{\mu'}\cdot\mathbf{Y}^{(\lambda)}_{LM}(\hat{\mathbf{k}}_0)[\mathbf{Y}^{(\lambda)}_{LM}(\hat{\mathbf{k}}_0)]^{*}\cdot\hat{\boldsymbol{\epsilon}}_{\mu}=(\mu\mu')^{(\lambda+1)}(8\pi)^{-1}(2L+1)\mathscr{D}^{(L)}_{\mu'M}(\hat{\mathbf{k}}_0,\hat{\mathbf{z}})[\mathscr{D}^{(L)}_{\mu M}(\hat{\mathbf{k}}_0,\hat{\mathbf{z}})]^{*}\ . \tag{A5}$$

Here the notation for the rotation matrices $\mathscr{D}$ is that of Rose[27] and $\mu,\mu'=\pm1$.

Finally, in the limit of no Zeeman splitting, the nuclear forward-scattering amplitude is diagonal for any orthogonal bases $\hat{\boldsymbol{\epsilon}}_a,\hat{\boldsymbol{\epsilon}}_b$, $(f_N)_{ab}=\delta_{ab}f_0/(x-i)$, where

$$f_0=\tfrac{1}{2}\hat{\lambda}e^{-k^2\langle x^2\rangle}\left[\frac{2J_1+1}{2J_0+1}\right]\left[\frac{\Gamma_\gamma}{\Gamma}\right]\ . \tag{A6}$$

[1]G. T. Trammell, in *Chemical Effects on Nuclear Transformations* (International Atomic Energy Agency, Vienna, 1961), Vol. I, p. 75.
[2]G. T. Trammell, Phys. Rev. **126**, 1045 (1962).
[3]P. J. Black and P. B. Moon, Nature (London) **188**, 481 (1960).
[4]S. Bernstein and E. C. Campbell, Phys. Rev. **132**, 1625 (1963).
[5]A. M. Afanas'ev and Yu. Kagan, Zh. Eksp. Teor. Fiz. **48**, 327 (1965) [Sov. Phys.—JETP **21**, 215 (1965)].

[6]Yu. M. Kagan, A. M. Afanas'ev, and I. P. Perstnev, Zh. Eksp. Teor. Fiz. **54**, 1530 (1968) [Sov. Phys.—JETP **27**, 819 (1968)].

[7]P. A. Alexandrov and Yu. Kagan, Zh. Eksp. Teor. Fiz. **59**, 1733 (1970) [Sov. Phys.—JETP **32**, 942 (1971)].

[8]J. P. Hannon and G. T. Trammell, Phys. Rev. **169**, 315 (1968).

[9]J. P. Hannon and G. T. Trammell, Phys. Rev. **186**, 306 (1969).

[10]J. P. Hannon, N. J. Carron, and G. T. Trammell, Phys. Rev. B **9**, 2791 (1974); **9**, 2810 (1974).

[11]Surveys of γ-ray diffraction with extensive experimental and theoretical references have been given by V. A. Belyakov (Usp. Fiz. Nauk **115**, 553 (1975) [Sov. Phys.—Usp. **18**, 267 (1975)]) and by P. C. Champeney [Rep. Prog. Phys. **42**, 1017 (1979)].

[12]G. T. Trammell, J. P. Hannon, S. L. Ruby, Paul Flinn, R. L. Mössbauer, and F. Parak, in *Workshop on New Directions in Mössbauer Spectroscopy (Argonne 1977)*, edited by G. J. Perlow (AIP, New York, 1978), pp. 46—49 (AIP Conf. Proc. No. 38).

[13]V. A. Belyakov and Ya. N. Aivazian, Zh. Eksp. Teor. Fiz. **56**, 346 (1969) [Sov. Phys.—JETP **29**, 191 (1969)]; Phys. Rev. B **1**, 1903 (1970).

[14]G. V. Smirnov, V. V. Sklyarevskii, R. A. Voskanyan, and A. N. Artem'ev, Zh. Eksp. Teor. Fiz. Pis'ma Red. **9**, 123 (1969) [JETP Lett. **9**, 70 (1969)].

[15]U. van Bürck, G. V. Smirnov, R. L. Mössbauer, H. J. Maurus, and N. A. Semioschkina, J. Phys. C **13**, 4511 (1980).

[16]H. Winkler, R. Eisberg, E. Alp, R. Rüffer, E. Gerdau, S. Lauer, A. X. Trautwein, M. Grodzicki, and A. Vera, Z. Phys. B **49**, 331 (1983).

[17]R. M. Mirzababaev, G. V. Smirnov, V. V. Sklyarevskii, A. N. Artem'ev, A. N. Izrailenko, and A. V. Bobkov, Phys. Lett. **37A**, 441 (1971).

[18]P. J. Black and J. P. Duerdoth, Proc. Phys. Soc. London **84**, 169 (1964).

[19]J. P. Hannon, G. T. Trammell, E. Gerdau, M. Mueller, R. Rüffer, and H. Winkler, Phys. Rev. B **32**, 5068 (1985), paper I; **32**, 5081 (1985), paper II.

[20]J. P. Hannon, G. T. Trammell, M. Mueller, E. Gerdau, H. Winkler, and R. Rüffer, Phys. Rev. Lett. **43**, 636 (1979).

[21]J. P. Hannon, G. T. Trammell, M. Mueller, E. Gerdau, R. Rüffer, and H. Winkler, following paper, Phys. Rev. B **32**, 6374 (1985) paper IV.

[22]J. P. Hannon, N. V. Hung, J. T. Hutton, G. T. Trammell, E. Gerdau, and R. Rüffer, (unpublished) (paper V).

[23]S. Bernstein, E. C. Campbell, and C. W. Nestor, Jr., J. Phys. Chem. Solids **26**, 883 (1965).

[24]F. E. Wagner, Z. Phys. **210**, 361 (1968).

[25]M. Blume and O. C. Kistner, Phys. Rev. **171**, 417 (1968).

[26]R. M. Housley, R. W. Grant, and V. Gonser, Phys. Rev. **178**, 514 (1969).

[27]M. E. Rose, *Elementary Theory of Angular Momentum* (Wiley, New York, 1957), pp. 32—48.

[28]M. Blume and J. A. Tjon, Phys. Rev. **165**, 446 (1968).

[29]A. M. Afanas'ev and V. D. Gorobchenko, Zh. Eksp. Teor. Fiz. **66**, 1406 (1974) [Sov. Phys.—JETP **39**, 690 (1974)].

[30]F. Gonzales-Jimenez, P. Imbert, and F. Hartmann-Boutron, Phys. Rev. B **9**, 45 (1974).

[31]G. K. Shenoy, B. D. Dunlap, S. Dattagupta, and L. Asch, Phys. Rev. Lett. **37**, 539 (1976); Phys. Rev. B **16**, 3893 (1977).

[32]Here $\delta\phi$ is measured from the actual Bragg, which has an index of refraction shift, rather than exact geometric Bragg.

[33]Note that

$$\beta_N=\frac{[1-(\phi_c/\phi)^2+in\lambda\sigma_e/\phi^2+n\lambda^2 f_N/\pi\phi^2]^{1/2}}{[1-(\phi_c/\phi)^2+in\lambda\sigma_e/\phi^2]^{1/2}} .$$

Each of these square-root factors has a positive imaginary part, but note that the imaginary part of β_N can have either sign.

[34]J. P. Hannon, J. T. Hutton, G. T. Trammell, E. Gerdau, and R. Rüffer (unpublished) (paper VI).